The International Journal of Geomechanics
Volume 2, Number 1, 113–134 (2002)

2D Finite Element Analysis of Multicomponent Contaminant Transport Through Soils

Daichao Sheng and David W. Smith

Received June 2, 2001

Department of Civil, Surveying and Environmental Engineering,
University of Newcastle, NSW 2308, Australia
e-mail: Daichao.Sheng@newcastle.edu.au

ABSTRACT. *This article presents a two-dimensional finite element method for the solution of the advection-dispersion transport equation for multicomponent contaminants. While the approach described is general, the analysis presented here is restricted to nonlinear, equilibrium-controlled sorption and exchange of soluble inorganic ions. The finite element method is based on a generalization of the one-dimensional Transport-Equilibrium Petrov–Galerkin (TEPG) methods presented by Sheng and Smith [1]. In the TEPG methods, the reaction term is treated as a part of the mass accumulation term. This is in contrast with common formulations where the reaction term is treated as a source term. The transport equation thus contains two unknowns, the aqueous concentration and the total analytical concentration. The solution strategy adopted is to solve the transport equations coupled with chemical equilibrium equations by sequential iteration. No assumption on the reaction term is required when solving the transport equation, which means the transport equation is always conservative. At the end of each time step, both the transport and chemical equilibrium equations are satisfied. To facilitate the solution of the transport equations that may be advection dominated, and optimal upwind weighting procedure and mid-point time stepping scheme are employed. A number of significant improvements are presented here beyond the TEPG methods presented by Sheng and Smith. These improvements included upwind weighting for a heterogeneous fluid velocity field, the solution of the chemical equilibrium equations for both adsorption and ion exchange, the introduction of an automatic time stepping scheme so as to maintain a predetermined accuracy, and the description of strategies to improve the efficiency of the numerical computations.*

The TEPG method described is used to analyse several problems with the Peclet number varying between zero and infinity. Both two-dimensional plane flow and axi-symmetric problems are considered. The method described is shown to be capable of predicting important qualitative features of advection-dispersion transport involving nonlinear chemical equilibrium equations. For example problems analyzed, the method is found to be robust, efficient, and accurate, and on the basis of these examples more detailed investigations are justified.

Key Words and Phrases. finite element method, multicomponent contaminant transport, advection, dispersion, nonlinear sorption, upwind weighting.

 DOI: 10.1061/(ASCE)1532-3641(2002)2:1(113)
ISSN 1532-3641

I. Introduction

Chemical and biological processes accompanying contaminant transport in soils may be described either by rate equations or equilibrium equations, or some combination of both. Biological processes in soils are often modeled as zero-order or first-order chemical kinetic equations, and these simple rate equations are usually substituted directly into the transport equations. In this case the solutions to the standard advection-dispersion equation remain linear, and established methods of solution are generally satisfactory for these cases.

Because the geochemical database on chemical kinetics is currently small and incomplete, most geochemical modeling is based on the assumption that all the chemical components are in equilibrium. Even with this simplification, the chemical equilibrium equations are strongly nonlinear [2, 3], and if the chemical equilibrium equations are substituted directly into the transport equations, the system of equations becomes from a practical viewpoint, unsolvable.

Further, the nonlinear chemical equations fundamentally alter the nature of the solutions to the advection-dispersion equation. For example, given an advection-dominated transport problem, the introduction of a nonlinear adsorption isotherm can create shock and rarefaction waves. Analytic solutions describing the elementary behaviors of these waveforms were investigated in the article by Sheng and Smith [4]. Processes involving shock and rarefaction waves are known to present many difficulties in their numerical representation. Further, given an advection-dispersion transport problem with multiple chemical components—for example, competition of the components for a limited number of sorption sites—can result in multiple peaks in the component concentrations [1, 5]. This behavior is not predicted by simple transport analyses that neglect cross-couplings between the chemical components. Therefore, it is clear that transport problems involving nonlinear multicomponent chemical equilibrium processes can significantly complicate the solution procedure.

Given these difficulties, it is perhaps not surprising that only a modest amount of research has been done on the development of accurate, robust, and efficient numerical algorithms for solving the advection-dispersion transport equations when coupled with nonlinear chemical equilibrium equations. Early work on modeling of these problems frequently used standard transport algorithms based on the Galerkin finite element method, or more usually the central finite difference method [6]–[10]. However, it is well known that these standard numerical methods for transport problems only work well for diffusion dominated problems [11]. For advection-dominated problems, they tend to oscillate and give inaccurate results, particularly for large time steps. Another important issue about accuracy and robustness is the convergence between the transport and equilibrium equations. If the two systems of equations are weakly coupled and solved separately (as recommended for the reason of efficiency [12] see below), it is generally required to have some sort of iteration between transport and chemical reaction. Explicit methods without any iteration tend to be oscillating and inaccurate, even if special techniques are used to handle advection dominance [1]. On the other hand, implicit methods are not always convergent [1]. For example, the iterative backward Euler method was found to have difficulty in reaching convergence between the transport and equilibrium equations [1].

The efficiency of a numerical method is usually measured by its requirement for CPU (Central Process Unit) memory and CPU time. Methods that require excessive CPU memory and CPU time by definition are difficult to use in practice. The efficiency concern becomes particularly relevant for multidimensional problems. As the number of unknowns are equal to the product of the number of nodes and the number of components, the analyst may end up with a tremendous number of equations to solve in a complex multidimensional space involving a great number of components. If these equations are solved simultaneously, the CPU requirement can be excessive. Yeh and Tripathi [12] addressed this issue and pointed out that the only practical strategy is to

solve the transport and equilibrium equations separately by so-called 'sequential iteration.' This sequential iteration approach has then been adopted in a number of numerical models, for example, Walter et al. [10] and Abrams and Loague [13].

More recently, Sheng and Smith [1] presented a characteristic finite element (CFE) method and a group of transport-equilibrium Petrov–Galerkin (TEPG) methods. These methods were all described for one-dimensional problems with a steady-state unidirectional fluid velocity. One main difference between the methods by Sheng and Smith [1] and other sequential iteration methods, such as by Walter et al. [10], is that the reaction term is treated as a part of the mass accumulation term instead of a source term. Therefore, no assumption on the reaction term is required when solving the transport equation, which means the transport equation is always conservative. At the end of each time step, both the transport equation and the set of chemical equilibrium equations are satisfied, which makes these methods very similar to the direct approach where the transport and equilibrium equations are solved simultaneously. Through extensive analyses of various problems with the Peclet number varying from zero to infinite, they found the CFE method and one of the TEPG methods are in general accurate, robust and efficient, The CFE method, which is essentially a Lagrangian method, was particularly accurate in predicting shock fronts. However, in the current version of the CFE method, a requirement of the method is the simultaneous solution of a system of coupled transport-equilibrium equations for all components at all nodes. The extension of this method to complex problems involving multiple dimensions therefore requires further research, particularly regarding improvements to its efficiency.

The TEPG method, which belongs to the Eulerian approach, uses the middle point time stepping scheme and the optimal upwind weighting procedure. This TEPG method is less accurate than the CFE method in predicting shock fronts, but is simpler to implement. It solves the transport and equilibrium equations separately and seeks the convergence between the two systems by iteration. Whit this feature, the TEPG method can be implemented so that it does not require excessive CPU memory or time as the numbers of nodes and components increase. It is for this reason that the TEPG method is found to be more efficient for multidimensional problems.

In this article, the TEPG method with a middle point time stepping scheme will be extended to problems in two spatial dimensions. A number of refinements are presented, including upwind weighting for a fluid velocity varying in space (or possibly in time), equilibrium equations describing ion exchange, automatic time stepping and strategies for efficiency improvements. Both two-dimensional plane flow and axi-symmetric problems are considered.

II. Transport-equilibrium Petrov–Galerkin method

A. Governing equations

In two spatial dimensions, the standard governing equation for contaminant transport in soils can be written in the following general form [14]

$$\frac{\partial C_i}{\partial t}+\frac{\rho_{\mathrm{d}}}{n}\frac{\partial S_i}{\partial t}=\frac{\partial}{\partial x}\left\{D_{xi}\frac{\partial C_i}{\partial x}\right\}+\frac{\partial}{\partial y}\left\{D_{yi}\frac{\partial C_i}{\partial y}\right\}-\frac{\partial}{\partial x}\left\{\frac{v_x}{n}C_i\right\}-\frac{\partial}{\partial y}\left\{\frac{v_y}{n}C_i\right\}-\lambda_i C_i-\varepsilon_i \quad (1)$$

where C is the concentration of a component in the pore fluid, S is the concentration of the component sorbed on the solid phase, D is the dispersion-diffusion coefficient, v is the mean pore fluid velocity through the porous medium, λ is a rate constant describing any first-order kinetic processes, ε is a constant describing any zero-order kinetic processes, n is the soil porosity, ρ_{d} is the dry density of the porous medium (i. e., the soil in this case), x and y denote the two spatial coordinates, t is the time, subscript i denotes component i, while subscripts x and y denotes the x and y directions, respectively. The concentration C in the pore fluid has units of mass per unit

volume of pore fluid. The concentration S on the solid phase has units of mass per unit mass of dry soil.

The rate of change of the concentration on the solid phase [i. e., $\partial S/\partial t$ in equation (1)], in general can be due to a number of chemical and biological processes, such as adsorption, ion exchange, dissolution, precipitation, and biodegradation. However, this article focuses on sorption and ion exchange processes only. A competitive Langmuir isotherm is often used to describe sorption for a multicomponent systems, [15, 16] viz,

$$S_i^{\mathrm{a}} = \frac{K_i C_i Q^{\mathrm{a}}}{1 + \sum_{j=1}^{Nos} K_j C_j} \tag{2}$$

where S^{a} is the concentration of a component on the solid phase due to adsorption, K is the adsorption parameter, Q^{a} is the maximum adsorption capacity of the solid Nos is the number of components, and subscripts i and j stand for the components i and j. Note that Q^{a} has the same unit as S_i and the unit of K_i is the inverse of the C_i units.

For ion exchange, the equilibrium equation generally involves component valences. For demonstration purposes, a constant separation factor is assumed after the method of Jeong and Lee [5]. They derived the following equation for ion exchange for multiple components as,

$$S_i^{\mathrm{e}} = \frac{\alpha_{ir} C_i Q^{\mathrm{e}}}{\sum_{j=1}^{Nos} \alpha_{jr} e_j C_j} \tag{3}$$

where S^{e} is the concentration on the solid phase due to ion exchange, α_{ir} is the separation factor between component i and a reference component r, Q^{e} is the ion exchange capacity of the solid, and e_j is the valence of component j. Note that Q^{e} has the same units as $(e_j\, S_j)$ and α_{ir} is a dimensionless parameter.

The total concentration on the solid phase for component i is then

$$S_i = S_i^{\mathrm{a}} + S_i^{\mathrm{e}} = \frac{K_i C_i Q^{\mathrm{a}}}{1 + \sum_{j=1}^{Nos} K_i C_i} + \frac{\alpha_{ir} C_i Q^{\mathrm{e}}}{\sum_{j+1}^{Nos} \alpha_{ir} e_j C_j} \tag{4}$$

B. Initial and boundary conditions

The initial condition is given in terms of the concentrations in the pore fluid;

$$C_i(x, y, 0) = C_i^0(x, y)\ . \tag{5}$$

It is usually assumed that the dissolved concentration C_i is initially in equilibrium with the sorbed concentration S_i. Therefore, the initial sorbed concentrations S_i can be found from (4).

The boundary conditions considered in this article include the prescribed concentrations and prescribed flux

$$C_i = G_i(t) \qquad \text{on } \Gamma_1 \tag{6}$$

$$-D_{xi}\frac{\partial C_i}{\partial x}\xi_x - D_{yi}\frac{\partial C_i}{\partial y}\xi_y + \left(\frac{v_x}{n}\xi_x + \frac{v_y}{n}\xi_y\right) C_i = q_i(t) \qquad \text{on } \Gamma_2 \tag{7}$$

where G_i and q_i are prescribed functions of time, Γ_1 and Γ_2 are boundaries of the domain of interest, and ξ_x and ξ_y are the direction cosines of the outward normal to boundary Γ_2.

C. Petrov–Galerkin method for the transport equation

In the TEPG method, the concentration change in the transport equation (1) are rewritten in terms of the total concentration T_i defined as

$$T_i = C_i + \frac{\rho_d}{n} S_i \ . \tag{8}$$

Substituting (8) into (1) leads to Nos independent equations in terms of T_i and C_i. To reduce CPU memory requirements, we can apply the Petrov–Galerkin weighting procedure to the transport equation for each component individually, and form and solve the discretized equations for each component. Now dropping the subscript i for simplicity of notation, the discretized global finite element equation for one single component take the form

$$\mathbf{M}\frac{\mathrm{d}\underline{\mathbf{T}}}{\mathrm{d}t} + \mathbf{H}\underline{\mathbf{C}} + \mathbf{F} = \mathbf{0} \tag{9}$$

where $\mathbf{M}$ is the global mass matrix, $\mathbf{H}$ is the global transport matrix, $\mathbf{F}$ is the global supply vector, $\underline{\mathbf{T}}$ and $\underline{\mathbf{C}}$ are discretized total and dissolved concentrations, respectively. The matrices $\mathbf{M}$ and $\mathbf{H}$ as well as the vector $\mathbf{F}$ are formed for each element and then assembled in a global matrix. For each element, these matrices and vectors take the form

$$M^{\mathrm{e}}_{mn} = \int_{\Omega^{\mathrm{e}}} W_m N_n \,\mathrm{d}x\,\mathrm{d}y \tag{10}$$

$$\begin{aligned} H^{\mathrm{e}}_{mn} = &\int_{\Omega^{\mathrm{e}}} \left\{ D_x \frac{\partial W_m}{\partial x}\frac{\partial N_n}{\partial x} + D_y \frac{\partial W_m}{\partial y}\frac{\partial N_n}{\partial y} \right\} \mathrm{d}x\,\mathrm{d}y + \int_{\Omega^{\mathrm{e}}} \left\{ \frac{v_x}{n} W_m \frac{\partial N_n}{\partial x} + \frac{v_y}{n} W_m \frac{\partial N_n}{\partial y} \right\} \mathrm{d}x\,\mathrm{d}y \\ &+ \int_{\Omega^{\mathrm{e}}} W_m \,\lambda N_n \,\mathrm{d}x\,\mathrm{d}y - \int_{\Gamma^{\mathrm{e}}} W_m \left(\frac{v_x}{n}\xi_x + \frac{v_y}{n}\xi_y \right) N_n \,\mathrm{d}\Gamma \end{aligned} \tag{11}$$

$$F^{\mathrm{e}}_m = \int_{\Omega^{\mathrm{e}}} W_m \varepsilon \,\mathrm{d}x\,\mathrm{d}y + \int_{\Gamma^{\mathrm{e}}} W_m \, q \,\mathrm{d}\Gamma \tag{12}$$

where M^{e}_{mn} is the local mass matrix for a single element, H^{e}_{mn} is the local transport matrix, F^{e}_m is the local supply vector, W_m is the weighting function at local node m, N_n is the shape function at local node n, Ω^{e} is the element area, Γ^{e} is the element boundary, subscripts m and n here stand for local node numbers. For a 3-noded triangular element, M^{e}_{mn} and H^{e}_{mn} are 3×3 matrices and F^{e}_m is a column vector of dimension 3. Note that the fluid velocity is assumed to be homogeneous inside each element in deriving equation (11).

In the equations above, we see that the local matrices $\mathbf{M}^{\mathrm{e}}$, $\mathbf{H}^{\mathrm{e}}$, and $\mathbf{F}^{\mathrm{e}}$, hence the global matrices $\mathbf{M}$, $\mathbf{H}$, and $\mathbf{F}$, are in general dependent on the particular component considered, as the weighting function W_m, the diffusivity D_x and D_y and the source terms λ and ε can be component specific. Therefore, it would significantly increase the requirement for CPU memory if $\mathbf{M}$, $\mathbf{H}$, and $\mathbf{F}$ were formed and stored for all components simultaneously. Instead, it is more efficient to form $\mathbf{M}$, $\mathbf{H}$, and $\mathbf{F}$ once per component and store them on scratch files for later use. For this reason we are required to repeat the calculations component by component. However, as the integrations in (11) and (12) are relatively easy to compute, this repetition will not significantly increase the CPU time.

Applying a θ scheme for time stepping to equation (9) leads to

$$\mathbf{M}\frac{\underline{\mathbf{T}}^{k+1} - \underline{\mathbf{T}}^{k}}{\Delta t} + \mathbf{H}\left((1-\theta)\underline{\mathbf{C}}^{k} + \theta\underline{\mathbf{C}}^{k+1} \right) + \mathbf{F}^{k+1} = \mathbf{0} \tag{13}$$

where Δt is the time step, θ is a parameter between 0 and 1, and superscripts k and $k+1$ stand for time level t_k and $t_{k+1} = t_k + \Delta t$, respectively. Given $\underline{\mathbf{C}}^{k}$ and $\underline{\mathbf{C}}^{k+1}$, equation (13) can be solved

for $\underline{\mathbf{T}}^{k+1}$. Again, it is more efficient to solve equation (13) Nos times for the Nos components than once for all components. The solution process for equation (13) as well as the choice of θ will be discussed later in this section.

D. Upwind weighting in two-dimensional space

For two spatial dimensions, the Petrov–Galerkin weighting function W in Equations (10) to (12) uses upwinding along the local element streamline. Similar to the simple discontinuous weighting function in Sheng and Smith [1], we have here

$$W_m = N_m + \frac{\xi \bar{l}_v}{2} \nabla_v N_m \tag{14}$$

where ξ is a parameter between 0 and 1. $\bar{l}_v$ is the characteristic length of the element in the direction of local fluid velocity. ∇_v is the gradient operator alone the streamline, subscript v, stands for the local fluid velocity vector defined as $\mathbf{v} = \{v_x, v_y\}^T$, and subscript m stands for local node m of the element. Substituting the vector $\mathbf{v}$ into equation (14) gives

$$W_i = N_i + \frac{\xi \bar{l}_v}{2} \left(\frac{v_x}{v} \frac{\partial N_i}{\partial x} + \frac{v_y}{v} \frac{\partial N_i}{\partial y} \right) \tag{15}$$

where $v = \sqrt{v_x^2 + v_y^2}$. The weighting function above is discontinuous at node points. As this discontinuity is treated inside each element, it will not cause infinity in the integration of the diffusion part of equation (11) [11].

The characteristic length $\bar{l}_v$ can be approximated by the average thickness of the element in the direction of the fluid velocity. To find this thickness, we may first transform the nodal coordinates (x_m, y_m) to the coordinates (x_{vm}, y_{vm}) defined by $\mathbf{v}$ and its perpendicular,

$$x_{vm} = \frac{v_x}{v} x_m + \frac{v_y}{v} y_m \tag{16}$$

$$y_{vm} = -\frac{v_y}{v} x_m + \frac{v_x}{v} y_m \, . \tag{17}$$

The length $\bar{l}_v$ can then be calculated as

$$\bar{l}_v = \frac{\Delta^{\mathrm{e}}}{\max(y_{vm}) - \min(y_{vm})} \tag{18}$$

where Δ^{e} is the area of the element, $\max(y_{vm})$ is the maximum nodal coordinate in y_{vm} and $\min(y_{vm})$ is the minimum nodal coordinate in y_{vm}.

The parameter ξ in equation (14) varies with the Peclet number and the following expression leads to the optimal weighting

$$\xi = \coth(Pe) - \frac{1}{Pe} \tag{19}$$

where Pe is the Pecler number. For two spatial dimensions, this number is defined as

$$Pe = \frac{v}{nD} \frac{\bar{l}_v}{2} = \frac{v}{n\sqrt{D_x^2 + D_y^2}} \frac{\bar{l}_v}{2} \, . \tag{20}$$

All the calculations in this subsection are performed element per element. This allows us to have different fluid velocities, dispersivities, and porosities for different elements. If the dispersivities or diffusivities D_x and D_y vary with components, the calculations also have to be repeated component after component. However, it is possible to choose the maximum Pe for all components for each element so that the calculations in this subsection need to be performed only once per element.

E. Direct iteration method for the equilibrium equations

With the total concentrations $\underline{\mathbf{T}}$ found from the solution of equation (9), the dissolved concentrations $\underline{\mathbf{C}}$ and the sorbed concentrations $\underline{\mathbf{S}}$ can then be solved from the equilibrium equations. Let us first write the equilibrium equation (4) in a more general form

$$S_i = S_i^{\mathrm{a}} + S_i^{\mathrm{e}} = f(C_1, C_2, \ldots, C_{Nos})\, C_i = f(C) C_i \ . \tag{21}$$

The function $f(C)$ can be determined by substituting Equations (2) and (3) into equation (21). Substituting equation (21) into equation (8) leads to, after some rearrangement,

$$C_i = \frac{T_i}{1 + \frac{\rho_{\mathrm{d}}}{n} f(C)} \ . \tag{22}$$

The equation above can be solved by direct iteration,

$$C_i^{k+1,s} = \frac{T^{k+1}}{1 + \frac{\rho_{\mathrm{d}}}{n} f\left(C^{k+1,s-1}\right)} \tag{23}$$

where superscript $(k+1, s)$ stands for iteration s at time level t_{k+1}. In the first iteration, function $f(C)$ can be estimated based on C^k at time level t_k. After each iteration, a relative error can be calculated for each node as

$$R_{\mathrm{c}} = \sqrt{\sum_{i=1}^{Nos} \left(C_i^{k+1,s} - C_i^{k+1,s-1}\right)^2 \Bigg/ \sum_{i=1}^{Nos} \left(C_i^{k+1,s}\right)^2} \tag{24}$$

where the Euclidean norm is used. The iteration stops once R_{c} is smaller than a prescribed tolerance *CTOL*. In general cases equation (23) converges very quickly and a stringent tolerance between $10^{-4} \sim 10^{-8}$ can be used here.

Once C^{k+1} is solved, S^{k+1} can be found from the equilibrium equation (4). The solution procedure discussed above can be applied node by node (i. e., solving the concentrations for all components at one node and then repeating the process for next node).

F. Iteration between the transport and equilibrium equations

If the time stepping parameter θ is set to 0, the transport and equilibrium equations are uncoupled and can be solved in a straightforward manner. At each time step, the transport equation is first solved for the total concentrations at all nodes for each component, and the equilibrium equations are then solved for the dissolved concentrations and the sorbed concentrations for all components at each node. However, Sheng and Smith [1] found that this explicit TEPG method is generally inaccurate and not stable.

For $\theta > 0$, iterations between the transport and equilibrium solutions are required, as the fluid concentrations $\underline{\mathbf{C}}^{k+1}$ are also unknown in equation (13). Sheng and Smith [1] found that

the implicit TEPG method with $\theta = 0.5$ performs best in the terms of convergence, accuracy and efficiency. Setting θ to 0.5 in equation (13) and rearranging terms give

$$\underline{\mathbf{T}}^{k+1} = \mathbf{M}^{-1}\left(\mathbf{M}\underline{\mathbf{T}}^{k} - \frac{1}{2}\Delta t\,\mathbf{H}\underline{\mathbf{C}}^{k} - \frac{1}{2}\Delta t\,\mathbf{H}\underline{\mathbf{C}}^{k+1} - \Delta t\mathbf{F}^{k+1}\right). \tag{25}$$

At each time step, we can first set $\underline{\mathbf{C}}^{k+1} = \mathbf{0}$ to start the iteration, and then solve equation (25) Nos times for the Nos components. The total concentrations obtained are stored as $\underline{\mathbf{T}}_1^{k+1}$ for iteration number 1. The equilibrium equations are then solved for $\underline{\mathbf{C}}^{k+1}$ and $\underline{\mathbf{S}}^{k+1}$. Substituting the obtained $\underline{\mathbf{C}}^{k+1}$ into equation (25) gives the total concentration $\underline{\mathbf{T}}_2^{k+1}$ for iteration number 2. This process is repeated until the difference in $\underline{\mathbf{T}}^{k+1}$ between two successive iterations becomes acceptable. The Euclidean norm can be used to define a relative error.

$$R = \left\|\underline{\mathbf{T}}_s^{k+1} - \underline{\mathbf{T}}_{s-1}^{k+1}\right\| \Big/ \left\|\underline{\mathbf{T}}_s^{k+1}\right\| \tag{26}$$

where the $\underline{\mathbf{T}}$ stores the total concentrations for all components at all nodes, subscript s stands for iteration s and superscript $k+1$ stands for time level t_{k+1}. For the first iteration $\underline{\mathbf{T}}_0$ can be set to $\mathbf{0}$. Once the relative error R is smaller than a prescribed tolerance *TTOL*, the iteration stops. If the relative error R does not converge to the tolerance *TTOL* within a prescribed number (*MAXIT*) of iteration permitted, the time step is adjusted according to

$$\Delta t_{\text{new}} = 0.9\sqrt{TTOL\,/\,R}\;\;\Delta t_{\text{old}} \tag{27}$$

where Δt_{new} is the new time step, and Δt_{old} is the time step that failed to give a convergent solution.

On the other hand, if the convergence ($R < TTOL$) is achieved within a small number of iterations (*SMLIT*), the time step can be increased according to

$$\Delta t_{\text{new}} = \min\left(1.1\sqrt{TTOL\,/\,R}\;\;\Delta t_{\text{old}},\;\; DT\right) \tag{28}$$

where Δt_{old} is the time step that succeeded in giving a convergence solution, and DT is the maximum time step allowed.

This automatic control of time steps based on a computed relative error is adapted from the subincrementation method for integrating stresses in displacement finite methods [17]. With this automatic time stepping, the actual sizes of prescribed time steps will only influence the efficiency but not the accuracy. In addition, the convergence is improved by this scheme and hence the finite element method of solution is more robust.

Because R is a global quantity representing an average value for all components at all nodes, only a moderate tolerance is suggested to be used here, for example, a *TTOL* between $10^{-2} \sim 10^{-4}$.

G. Axisymmetric problems

A special form of the two-dimensional transport equation (1) is the axi-symmetric problem. In this case, the governing equation can be written as

$$r\frac{\partial C_i}{\partial t} + r\frac{\rho_{\text{d}}}{n}\frac{\partial S_i}{\partial t} = \frac{\partial}{\partial r}\left\{r D_{ri}\frac{\partial C_i}{\partial r}\right\} + \frac{\partial}{\partial z}\left\{r D_{zi}\frac{\partial C_i}{\partial z}\right\} - \frac{\partial}{\partial r}\left\{\frac{v_r}{n} r C_i\right\} - \frac{\partial}{\partial z}\left\{\frac{v_z}{n} r C_i\right\} - r\,\lambda_i C_i - r\varepsilon_i \tag{29}$$

where r is the radial coordinate, z is the axial coordinate. Equation (29) can be reduced to Equation (1) if the coefficients in (29) are substituted by the modified coefficients $a' = r\,a$, with a denoting 1, $\frac{\rho_d}{n}$, D_r, D_z, $\frac{v_x}{n}$, $\frac{v_y}{n}$, λ and ε, respectively. With this substitution, the only change needed for an axi-symmetric problem is to compute the modified coefficients and use these coefficients when computing the element matrices.

H. Algorithm

The TEPG method described above can now be summarized in the following pseudo code:

1. Enter geometric, material, flow and time properties as well as initial and boundary conditions.
2. Enter the local equilibrium tolerance *CTOL*, the global convergence tolerance *TTOL*, the maximum global iterations *MAXIT* allowed per time step, and the maximum global iterations *SMLIT* allowed to increase the time step.
3. Enter the Courant number for time stepping.
4. Do Steps 5 to 6 for each element.
5. Compute and store element properties like the area, the characteristic length $\bar{l}_v$, the Peclet number Pe, and the upwind parameter ξ. If the element is axisymmetric, also compute the modified coefficients.
6. Compute and store the shape function N_j and its derivatives $\frac{\partial N_j}{\partial x}$ and $\frac{\partial N_j}{\partial y}$ for each node of the element.
7. Do Steps 8 to 12 for each component.
8. Do Steps 9 to 11 for each element.
9. Compute the weighting function W_j and its derivatives $\frac{\partial W_j}{\partial x}$ and $\frac{\partial W_j}{\partial y}$ for each node of the element.
10. Compute the element matrices and vectors $\mathbf{m}^e$, $\mathbf{h}^e$, and $\mathbf{f}^e$.
11. Assemble the element matrices to the global matrices $\mathbf{M}$, $\mathbf{H}$, and $\mathbf{F}$.
12. Store the global matrices $\mathbf{M}$, $\mathbf{H}$, and $\mathbf{F}$ for the component on scratch files.
13. Compute the initial sorbed concentrations $\underline{\mathbf{S}}^0$ according to the initial dissolved concentrations $\underline{\mathbf{C}}^0$.
14. Compute the initial total concentration $\underline{\mathbf{T}}^0 = \underline{\mathbf{C}}^0 + \underline{\mathbf{S}}^0$.
15. Compute the time step Δt according to the given Courant number. Store Δt to DT.
16. Set $k = 0$ and $t = 0$.
17. While $t < t_f$, do Steps 18 to 35.
18. Do Steps 19 to 21 for each component.
19. Retrieve the global matrices $\mathbf{M}$, $\mathbf{H}$, and $\mathbf{F}$ from the scratch files.
20. Update $\mathbf{F}$ according to the boundary conditions during $\left[t^k, t^k + \Delta t\right]$.
21. Solve the total concentration $\underline{\mathbf{T}}_2^{k+1}$ according to

$$\underline{\mathbf{T}}_2^{k+1} = \mathbf{M}^{-1}\left(\mathbf{M}\underline{\mathbf{T}}^k - \Delta t\mathbf{H}\underline{\mathbf{C}}^k - \Delta t\mathbf{F}\right) .$$

22. Solve the equilibrium equations for $\underline{\mathbf{C}}^{k+1}$ and $\underline{\mathbf{S}}^{k+1}$.
23. Set $\underline{\mathbf{T}}_1^{k+1} = \mathbf{0}$ for all components.
24. Set iteration count $ITER = 0$.
25. Do Steps 26 to 28 for each component.

26. Retrieve the global matrices **M**, **H**, and **F** from the scratch files.
27. Update **F** according to the boundary conditions during $[t^k, t^k + \Delta t]$.
28. Solve the total concentration $\underline{\mathbf{T}}_2^{k+1}$ according to

$$\underline{\mathbf{T}}_2^{k+1} = \mathbf{M}^{-1}\left(\mathbf{M}\underline{\mathbf{T}}^k - \frac{1}{2}\Delta t\mathbf{H}\underline{\mathbf{C}}^k - \frac{1}{2}\Delta t\mathbf{H}\underline{\mathbf{C}}^{k+1} - \Delta t\mathbf{F}\right) .$$

29. Solve the equilibrium equations for $\underline{\mathbf{C}}^{k+1}$ and $\underline{\mathbf{S}}^{k+1}$.
30. Set iteration counts $ITER = ITER + 1$.
31. Compute the norm

$$R = \left\|\underline{\mathbf{T}}_2^{k+1} - \underline{\mathbf{T}}_1^{k+1}\right\| \Big/ \left\|\underline{\mathbf{T}}_2^{k+1}\right\| .$$

32. If $R \leq TTOL$, go to Step 35.
33. Else if $ITER < MAXIT$, set $\underline{\mathbf{T}}_1^{k+1} = \underline{\mathbf{T}}_2^{k+1}$ and go to Step 25.
34. Else, compute the new time step according to

$$\Delta t = 0.9\sqrt{TTOL\ /R}\ \Delta t$$

and then go to Step 18.

35. If $ITER < SMLIT$, compute

$$\Delta t = \min\left(1.1\sqrt{TTOL\,/\,R}\ \ \Delta t,\ DT\right) .$$

36. Set

$$t = t + \Delta t$$
$$k = k + 1 .$$

In the pseudo code above, $\underline{\mathbf{T}}$, $\underline{\mathbf{C}}$, and $\underline{\mathbf{S}}$ store the concentrations for all components at all nodes, the global matrices,**M**, **H**, and **F** are used once per component, and t_f is the final time of interest. The solution of the equilibrium equations in Steps 22 and 29 follows for direct iteration methods discussed earlier and is not detailed in the code above.

III. Applications

The algorithm described above has been implemented on a personal computer and the code is given the name FETECS (Finite Elements for Transport and Equilibrium of Competitive Species). The code also includes the 1-D TEPG methods described in Sheng and Smith [1]. At present, only linear elements are used and these include 1-D rod elements, 2-D plane flow triangular elements and 2-D axisymmetric triangular elements. The code also features user-defined iteration tolerances, so that the convergence requirement can be problem specific.

In this section, a number of examples are analyzed using the 2-D TEPG method. In all the analyses that follow, the local equilibrium tolerance *CTOL* is set to 10^{-5} and the global convergence tolerance *TTOL* is set to 10^{-2}. The maximum global iterations *MAXIT* allowed for each time step is set to 100. The maximum iterations *SMLIT* below which the time step is allowed to increase is set to 3. The coarse time steps used in the analyses are determined according to a preset Courant number as

$$\Delta t = \begin{cases} Cr \min\left(\frac{nl_v}{v}\right) & Pe \geq 0.5 \\ Cr \min\left(\frac{l_v^2}{D}\right) & Pe < 0.5 \end{cases}$$

where the minimum values are taken over all elements. The Courant number Cr is set to 1 in all the analyses that follow, unless stated otherwise.

A. Column experiment of 4 components

The first example simulates the column experiment conducted by Jeong and Lee [5]. In this test, a soil column was first treated with a solution containing three ionic components Na^+, Mg^{2+}, and Ca^{2+} (all in chlorides). After the initial concentrations of these ions were established, a solution that contains an additional ionic component Co^{2+} (cobalt) was fed into the column with a constant volumetric flow rate. The initial and feed concentrations are listed in Table 1. The volumetric flow rate is 0.43 mL/(cm^2 min) and this corresponds to the Darcian velocity. The soil properties are given as follows: $n = 0.45$, $\rho_d = 1.0$ kg/cm^3, $Q^a = 5.94$ mmol/kg and $Q^e = 12.04$ meq/kg. Note here that the adsorption capacity and the ion exchange capacity are measured per kg of the dry soil mass. The adsorption parameters as well as the separation factors for each ions are listed in Table 1. No kinetic process is considered in this example.

TABLE 1

Initial and Feed Concentrations and Equilibrium Parameters

Components	Initial concentrations, mmol/L	Feed concentrations, mmol/L	Adsorption parameters, K_i, 1/mmol	Separation factor[#], α_{ir} 1/meq
Na^+	1	1	0.12	0.85
Mg^{2+}	1	1	0.11	1.28
Ca^{2+}	1	1	0.14	1.50
Co^{2+}	0	1	0.18	1.73

[#] H^+ is used as the reference components for the separation factor.

We can use the two-dimensional finite element formulation to solve this essentially one-dimensional problem. The soil column, which is 1.25 cm in radius and 40 cm in height, is represented by 400 axi-symmetric linear triangular elements. The elements used here are relatively small, the intention being to capture the shock fronts (see Figure 1). The Courant number is set to 2, in order to reduce the total number of time steps.

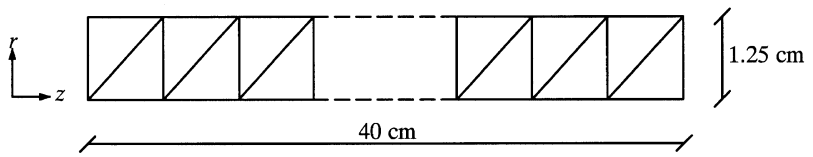

FIGURE 1 Mesh for the column test, 402 nodes and 400 (3-noded) elements.

Le us first assume there is no dispersion in the soil column. In this case, the analytical solution can be obtained from the theories of multicomponent chromatography [18] as described in Jeong and Lee [5]. For this advection problem, the three *in situ* components Na^+, Mg^{2+}, and Ca^{2+} travel in five concentration plateaus (four shock fronts), while the added component Co^{2+}

travels in two plateaus (one shock front). The analytical solution is shown in Figure 2, where the effluent concentrations are plotted against the total effluent volume. The numerical results, which are also shown in Figure 2, match the analytical concentrations very well, with distinct five plateaus in Na^+, Mg^{2+}, and Ca^{2+} and two plateaus in Co^{2+}. A clear 'calcium halo,' due to the liberation of Ca^{2+} from exchange sites, can be observed in Figure 2. However, it is noted that the shock fronts, particularly the last three, are somewhat smoothed in the numerical results.

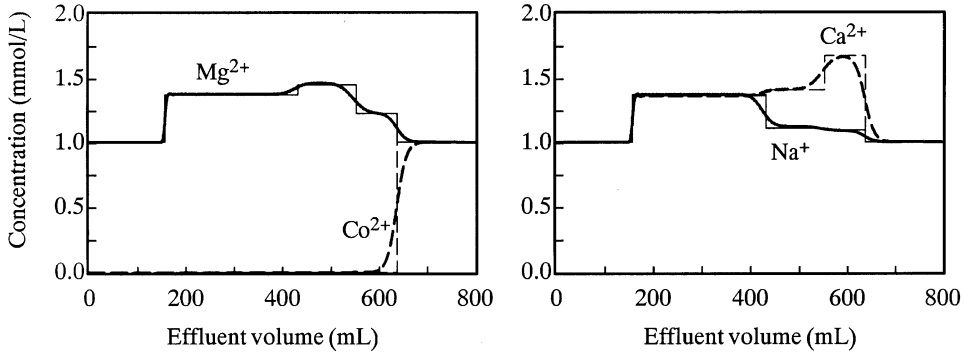

FIGURE 2 Numerical results (thick lines) versus analytical solutions (thin lines) for the column test (pure advection).

In order to see the effect of the time step size, the same problem is recomputed with a Courant number of 4. With either $Cr = 4$ or $Cr = 2$, no time step failed to reach convergence within 100 global iterations. Therefore, the time steps used in the two cases are uniform (i. e., $\Delta t = 0.4186$ for $Cr = 2$ and $\Delta t = 0.8372$ for $Cr = 4$). The results for $Cr = 4$ are compared with those for $Cr = 2.0$ in Figure 3. It can be seen that the Courant number or the time step size does not significantly influence the numerical results. Indeed, the concentrations obtained from the two Courant numbers are almost identical, except at the last shock front where slightly sharper gradients in Ca^{2+} and Co^{2+} are observed for $Cr = 2$.

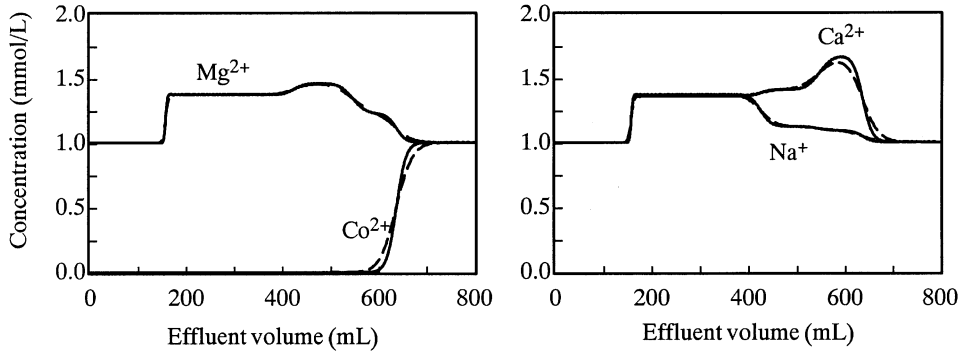

FIGURE 3 Effect of time step size on the numerical results (solid lines: $Cr = 2$, dashed line: $Cr = 4$, pure advection).

We can also introduce dispersion into this example. Let $D_r = D_z = 0.1$, which gives a local Peclet number of 0.5 approximately. The numerical results for this case are shown in Figure 4 and

are compared with the experimental results obtained by Jeong and Lee [5]. It can be noted that the predicted concentrations match the experimental results relatively well for large effluent volumes. The predicted patterns of the effluent concentration history are similar to the experimental ones. The predicted 'calcium halo' is almost identical to the observed one. However, discrepancies are observed for small effluent volumes. One possible reason for these discrepancies is the incomplete sorption equilibrium [5].

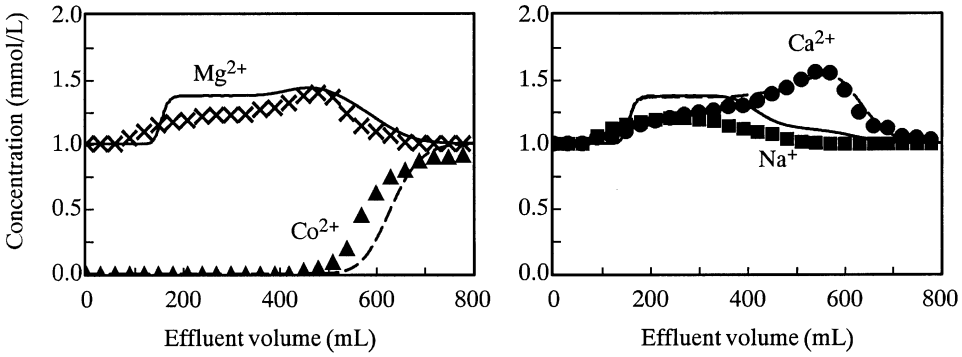

FIGURE 4 Numerical (lines) versus experimental (points) results for column test (advection and diffusion).

The convergence rate for this example is relatively fast. With global tolerance $TTOL = 10^{-2}$, it typically requires two or three global iterations for each successful time step. In the case of pure advection, there is no failed time step. In the case of advection and diffusion, the number of failed steps is 61, compared to the total 1010 steps. With the local tolerance $CTOL = 10^{-5}$, the maximum local iterations for the equilibrium equations varies between 18 and 25 with time steps.

B. Two-dimensional adsorption and desorption

In this example, we simulate a two-dimensional plane flow problem. The geometry of the problem is shown in Figure 5. An area, 2 units in depth and 10 units in length, consists of three soils that are marked by A, B, and C in Figure 5, respectively. This area is divided into 420 nodes and 738 triangular elements. The small elements along the soil interfaces use averaged material properties.

Initially, there is a uniform distribution of Component 1 in all the three soils. At time $t = 0$, Component 2 is added to the domain by applying a constant concentration at the top of Soil A. The transport in Soil A is dominated in the vertical $(-y)$ direction, while in Soil B in the horizontal $(+x)$ direction. In Soil C, the fluid velocity is generally zero, with possible diffusion in all directions. It is noted that the fluid velocities used in this example are hypothetical and do not satisfy continuity. The material properties as well as the flow condition are given in Table 2.

Three different cases are considered in Table 2. In Case I, only advection occurs and the Peclet number is infinite in all three soils. In Case II, both advection and diffusion occur and the local Peclet number is 0.5 in Soil A and Soil B, and 0 in Soil C. In Case III, the fluid velocity is uniformly zero and diffusion occurs in all three soils.

Only adsorption is considered in this example. The added component (Component 2) has a larger adsorption parameter than the *in situ* component (Component 1), with $K_2 = 10$ and

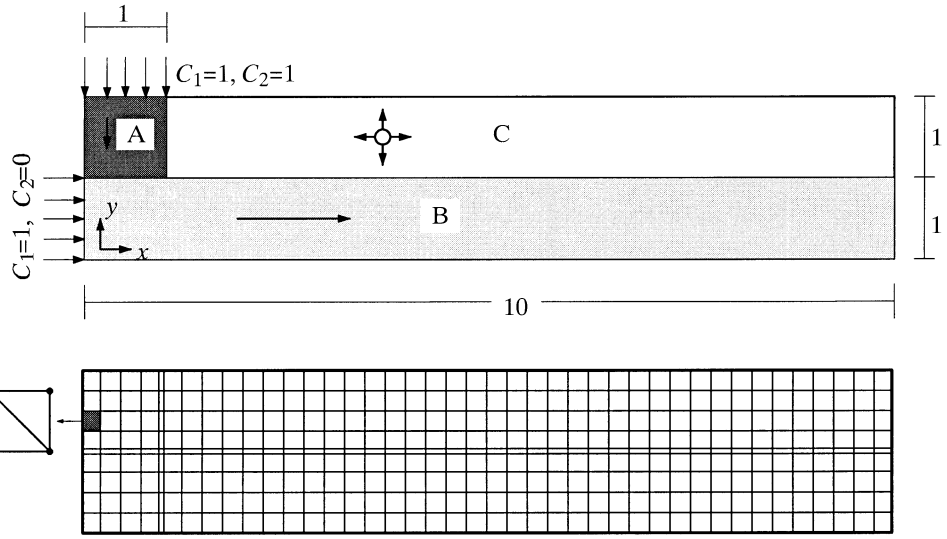

FIGURE 5 Two-dimensional advection-diffusion problem (totally 420 nodes and 738 triangular elements, the small elements along the soil interfaces use averaged material properties).

TABLE 2

Parameters Used for the Two-Dimensional Advection-Diffusion Problems

Cases	Properties	Soil A	Soil B	Soil C
	Physical	$n = 0.5, \varrho_d = 1.0$	$n = 0.5, \varrho_d = 1.0$	$n = 0.5, \varrho_d = 1.0$
	Fluid velocity	$v_x = 0,\ v_y = -1$	$v_x = 1,\ v_y = 0$	$v_x = 0,\ v_y = 0$
I	Diffusivity[#]	$D_x = 0,\ D_y = 0$	$D_x = 0,\ D_y = 0$	$D_x = 0,\ D_y = 0$
	Adsorption	$K_1 = 1,\ K_2 = 10,\ Q^a = 1$	$K_1 = 1,\ K_2 = 10,\ Q^a = 1$	$K_1 = 1,\ K_2 = 10,\ Q^a = 1$
	Ion exchange	$\alpha_1 = 0,\ \alpha_2 = 0,\ Q^e = 0$	$\alpha_1 = 0,\ \alpha_2 = 0,\ Q^e = 0$	$\alpha_1 = 0,\ \alpha_2 = 0,\ Q^e = 0$
	Kinetics	$\lambda_1 = \lambda_2 = 0,\ \varepsilon_1 = \varepsilon_2 = 0$	$\lambda_1 = \lambda_2 = 0,\ \varepsilon_1 = \varepsilon_2 = 0$	$\lambda_1 = \lambda_2 = 0,\ \varepsilon_1 = \varepsilon_2 = 0$
II	Physical	$n = 0.5, \varrho_d = 1.0$	$n = 0.5, \varrho_d = 1.0$	$n = 0.5, \varrho_d = 1.0$
	Fluid velocity	$v_x = 0,\ v_y = -1$	$v_x = 1,\ v_y = 0$	$v_x = 0,\ v_y = 0$
	Diffusivity[#]	$D_x = 0.25,\ D_y = 0.25$	$D_x = 0.25,\ D_y = 0.25$	$D_x = 0.1,\ D_y = 0.1$
	Adsorption	$K_1 = 1,\ K_2 = 10,\ Q^a = 1$	$K_1 = 1,\ K_2 = 10,\ Q^a = 1$	$K_1 = 1,\ K_2 = 10,\ Q^a = 1$
	Ion exchange	$\alpha_1 = 0,\ \alpha_2 = 0,\ Q^e = 0$	$\alpha_1 = 0,\ \alpha_2 = 0,\ Q^e = 0$	$\alpha_1 = 0,\ \alpha_2 = 0,\ Q^e = 0$
	Kinetics	$\lambda_1 = \lambda_2 = 0,\ \varepsilon_1 = \varepsilon_2 = 0$	$\lambda_1 = \lambda_2 = 0,\ \varepsilon_1 = \varepsilon_2 = 0$	$\lambda_1 = \lambda_2 = 0,\ \varepsilon_1 = \varepsilon_2 = 0$
III	Physical	$n = 0.5, \varrho_d = 1.0$	$n = 0.5, \varrho_d = 1.0$	$n = 0.5, \varrho_d = 1.0$
	Fluid velocity	$v_x = 0,\ v_y = 0$	$v_x = 0,\ v_y = 0$	$v_x = 0,\ v_y = 0$
	Diffusivity[#]	$D_x = 0.25,\ D_y = 0.25$	$D_x = 0.25,\ D_y = 0.25$	$D_x = 0.25,\ D_y = 0.25$
	Adsorption	$K_1 = 1,\ K_2 = 10,\ Q^a = 1$	$K_1 = 1,\ K_2 = 10,\ Q^a = 1$	$K_1 = 1,\ K_2 = 10,\ Q^a = 1$
	Ion exchange	$\alpha_1 = 0,\ \alpha_2 = 0,\ Q^e = 0$	$\alpha_1 = 0,\ \alpha_2 = 0,\ Q^e = 0$	$\alpha_1 = 0,\ \alpha_2 = 0,\ Q^e = 0$
	Kinetics	$\lambda_1 = \lambda_2 = 0,\ \varepsilon_1 = \varepsilon_2 = 0$	$\lambda_1 = \lambda_2 = 0,\ \varepsilon_1 = \varepsilon_2 = 0$	$\lambda_1 = \lambda_2 = 0,\ \varepsilon_1 = \varepsilon_2 = 0$

[#] Hydrodynamic dispersion coefficient.

$K_1 = 1$. The total adsorption capacities of the three soils are all set to 1 unit.

The boundary conditions for Case I and II are shown in Figure 5. At the top of Soil A, the dissolved concentrations of Component 1 and 2 are both set to 1 unit. This represents an injection boundary for Component 2. At the left (upstream) boundary of Soil B, the concentration of Component 1 is set to 1 and the concentration of Component 2 is set to 0. This represents a dissolution boundary for Component 2. Along all other inflow and no-flow boundaries of the area, the diffusive flux (q) is set to 0. In Case III where the fluid velocity is set to 0 uniformly,

the dissolution boundary in Soil B is removed, with other boundary conditions kept the same as Case I and II. The initial dissolved concentration C_1 of Component 1 is set to 1 in all the three soils, while the initial dissolved concentration C_2 for Component 2 is set to 0 uniformly. It is assumed that the sorbed concentrations S_1 and S_2 are initially in equilibrium with the dissolved concentrations C_1 and C_2, respectively.

In Case I where pure advection occurs, the computed concentrations are shown in Figure 6 to Figure 8 for different times. In Figure 6 where $t = 1$, the injected Component 2 competes with the *in situ* Components 1 in Soil A. As the concentration C_2 flows in [Figure 6(a)], S_2 takes up most of the adsorption sites of Soil A [Figure 6(c)]. The sorbed concentration S_1 decreases [Figure 6(d)]. This desorption of S_1 leads to an increase in the dissolved concentration C_1 [Figure 6(b)]. The peak of C_1 takes place at the downstream side of the concentration fronts of C_2 and S_2. This peak of C_1 thus in turn results in a peak in S_1 [Figure 6(d)]. In Figure 6(b) and Figure 6(d), we see that the peaks in C_1 and S_1 are just about to move into Soil B, while the fronts in C_2 and S_2 are still in Soil A.

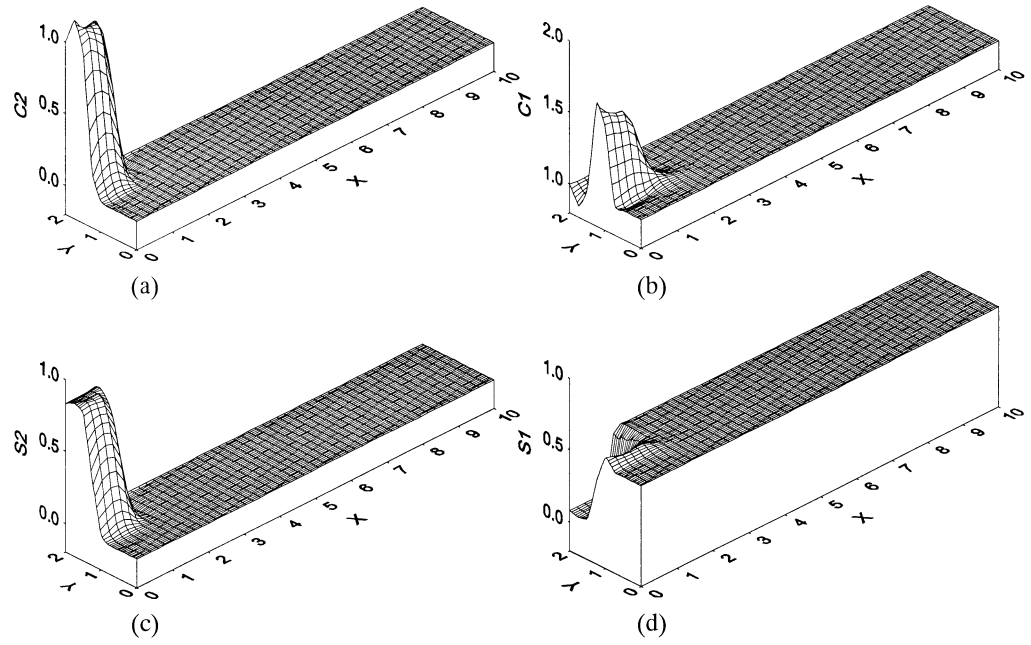

FIGURE 6 Case I: Pure advection, concentrations at time $t = 1$.

At time $t = 5$, the injected Component 2 has reached Soil B [Figure 7(a) and Figure 7(c)]. However, due to the dissolution effect at the upstream boundary of Soil B, the concentration fronts of C_2 and S_2 cannot reach the bottom of Soil B. The sorbed Component 1 is removed along the upper part of Soil B, creating an 'open channel' in the 3-D plot [Figure 7(d)]. The dissolved concentration C_1 displays a larger mound and the peak has completely moved into Soil B [Figure 7(b)].

At time $t = 10$, the concentrations C_2 and S_2 for the injected component form a 'thin wall' along the upper boundary of Soil B [Figure 8(a) and Figure 8(c)]. The 'open channel' in the sorbed concentration S_1 in Soil B becomes longer [Figure 8(d)] and the mound in the

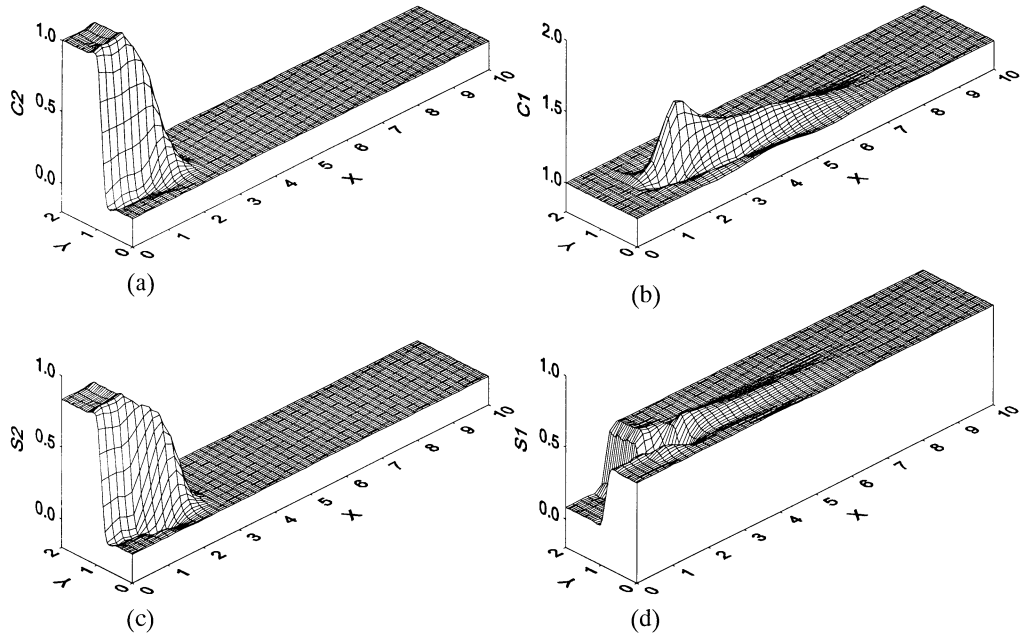

FIGURE 7 Case I: Pure advection, concentrations at time $t = 5$.

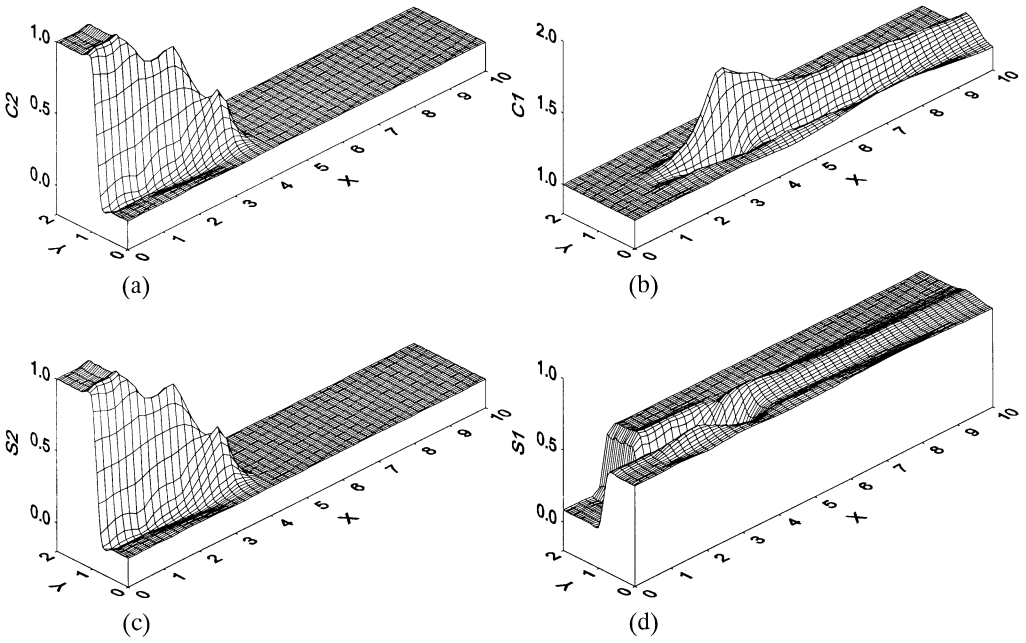

FIGURE 8 Case I: Pure advection, concentrations at time $t = 10$.

dissolved concentration C_1 reaches the downstream boundary of Soil B [Figure 8(b)]. In Soil A, the concentrations of the two components have reached a new steady state, i. e., $C_1 = C_2 = 1$, $S_1 = 0.083$, and $S_2 = 0.833$.

The results predicted by the TEPG method for this case generally make sense. The predicted peak and steady state concentrations also appear accurate. The convergence rate between the transport and equilibrium is relatively fast, with totally 335 iterations for 160 time steps. With $Cr = 1$, there is no failed time step. However, the TEPG is not capable of capturing sharp concentration fronts exactly and the positions of these fronts are only approximately correct. As advection is the only transport mechanism in this case and no rarefaction waves develop, the concentrations should travel in sharp fronts (shock waves). From Figure 6 to Figure 8, we see that the TEPG indeed introduces numerical diffusion at the shock fronts and these fronts are clearly smoothed. As the numerical diffusion essentially comes from nodal interpolation, it is only possible to reduce the smoothing effect by using very small elements, not necessarily by using small time steps.

The results for Case II are shown in Figure 9 to Figure 11. In this case, both advection and diffusion occur in Soil A and B, but only diffusion occurs in Soil C. At time $t = 1$, the

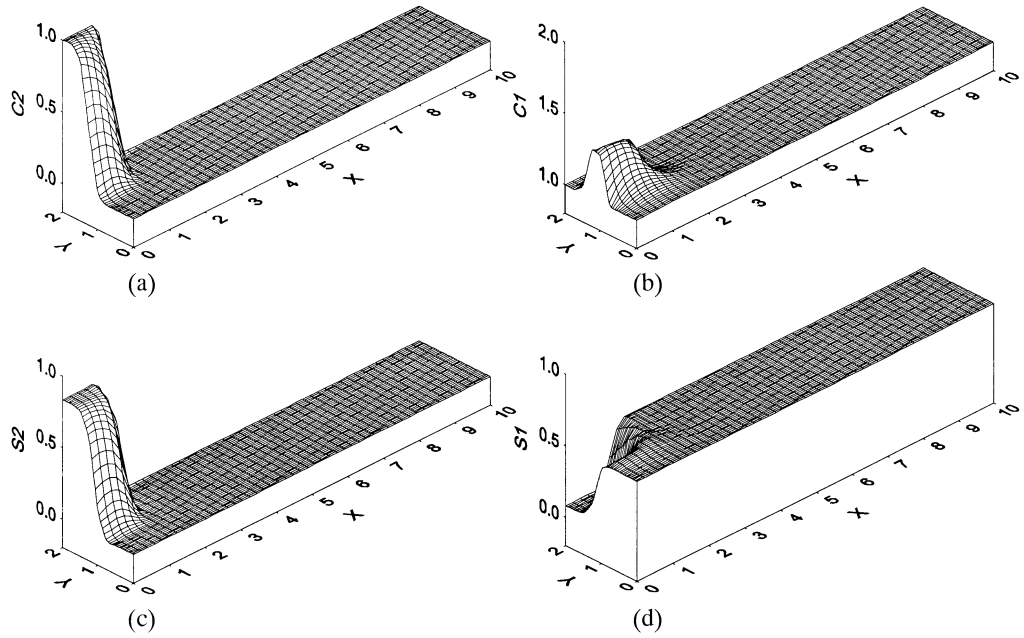

FIGURE 9 Case II: Advection and diffusion, concentrations at time $t = 1$.

results in Figure 9 are similar to those in Figure 6 for the pure advection case, except that the peak concentration in C_1 in Figure 9(b) is lower than that in Figure 6. As the time increases to 5, the concentrations in Figure 10 display some clearly different patterns from those in Figure 7. The concentrations C_2 and S_2 for the injected component reach the bottom of Soil B [Figure 10(a) and Figure 10(c)], despite the upstream dissolution boundary. The 'open channel' effect observed in the sorbed concentration S_1 in Case I is not obvious in Figure 10(d). The mound in the dissolved concentration C_1 is relatively low, but extended to a larger area including Soil C [Figure 10(b)].

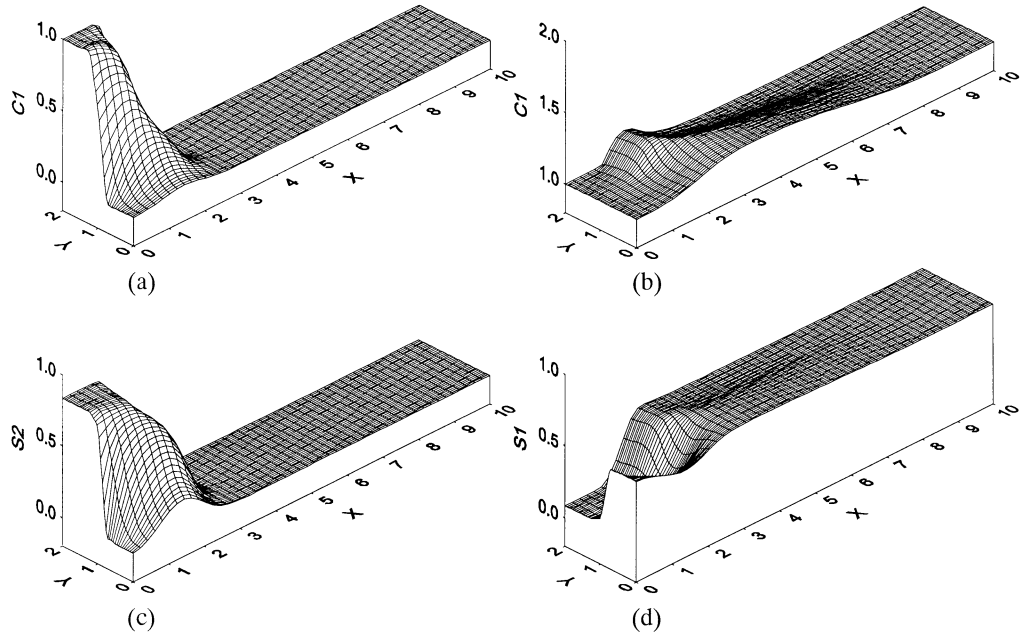

FIGURE 10 Case II: Advection and diffusion, concentrations at time $t = 5$.

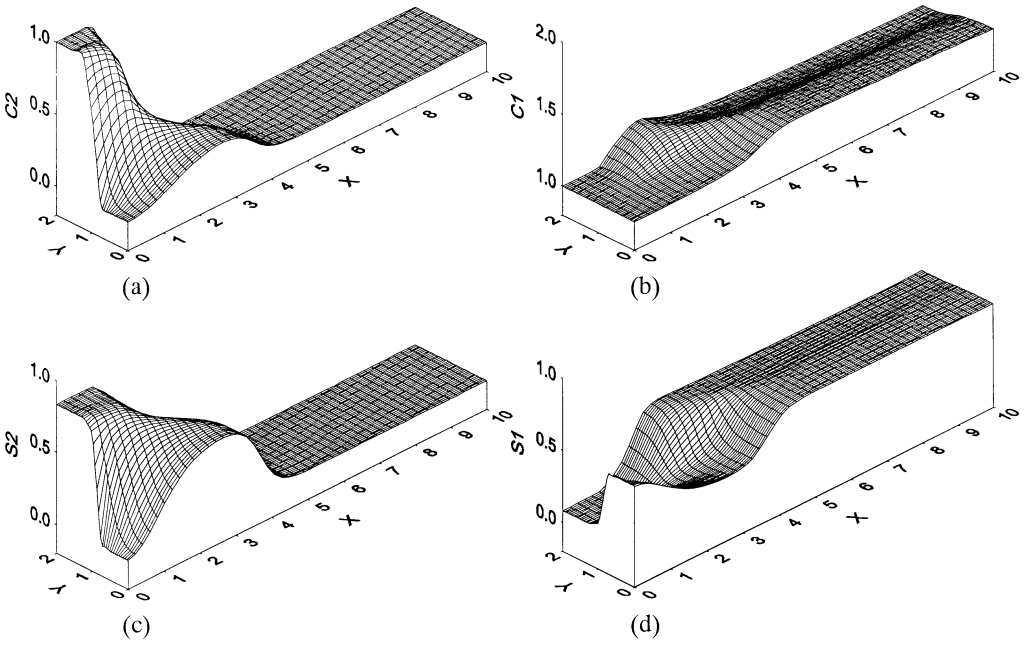

FIGURE 11 Case II: Advection and diffusion, concentrations at time $t = 10$.

At time $t = 10$, a significant amount of Component 2 has been diffused into Soil B [Figure 11(a) and Figure 11(c)], and a significant amount of sorbed concentration of Component 1 has been removed from Soil B [Figure 11(d)]. The mound in the dissolved concentration of Component 1 reaches the downstream boundary of Soil B and also diffuses to Soil C from its lower boundary [Figure 11(b)].

The convergence rate for Case II is slightly faster than Case I, with totally 322 global iterations for 160 time steps. The maximum local iterations vary between 13 to 15 with time steps. In this case, it is difficult to distinct the true diffusion and the numerical diffusion. However, as the numerical diffusion is mainly due to interpolation at sharp gradients and in this case these sharp gradients should already be smoothed by the true diffusion, the effect of the numerical diffusion should not be significant. This can also be confirmed through test runs using reduced diffusivities. It is expected that the diffusion effect will not decrease any further once the diffusivity is reduced to a certain value.

In case III where only diffusion occurs, the results obtained are shown in Figure 12 to Figure 14. Since there is no dissolution effect at the upstream boundary of Soil B, the added

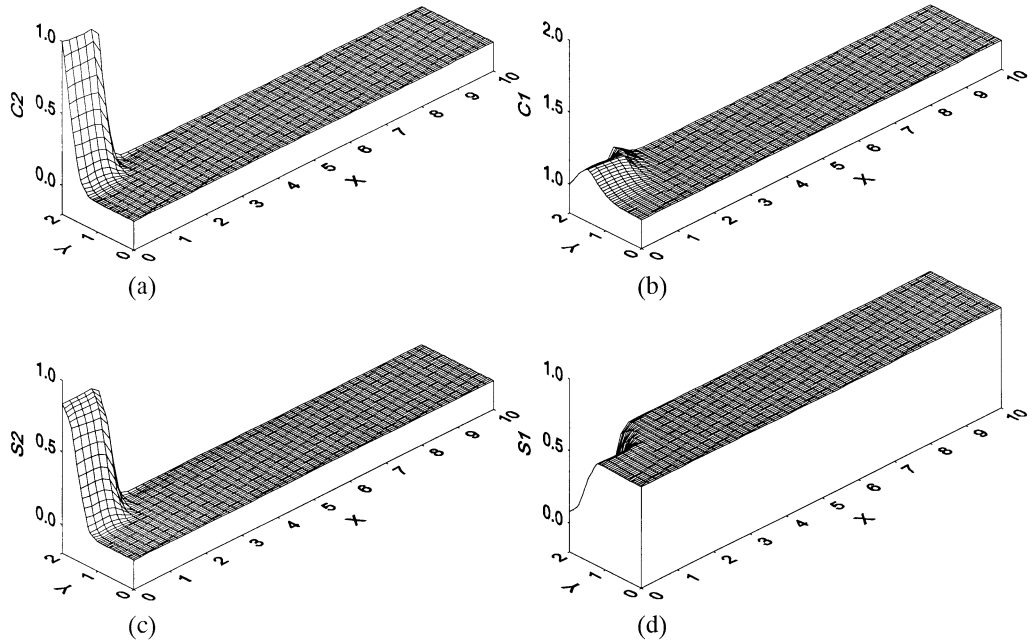

FIGURE 12 Case III: Pure diffusion, concentrations at time $t = 1$.

component diffuses at the same rate in Soil A and Soil B. The diffusion rate in Soil C is slower due to smaller diffusivity. The mound in the dissolved concentration of the *in situ* component is noticeable [Figure 12(b), Figure 13(b), and Figure 14(b)], and the peak values in C_1 distribute along a part of an ellipsis in the x-y plane.

The convergence rate for Case III is the fastest among the three cases, with typically only 1 global iteration per time step. The maximum local iterations for the equilibrium equations varies between 12 to 13, with $CTOL = 10^{-5}$.

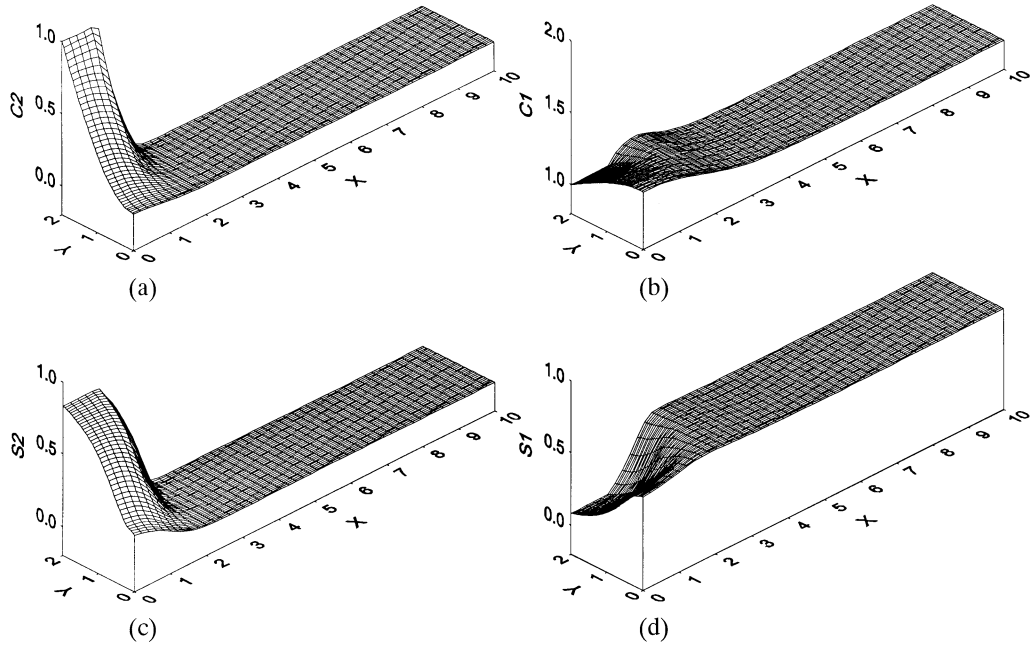

FIGURE 13 Case III: Pure diffusion, concentrations at time $t = 5$.

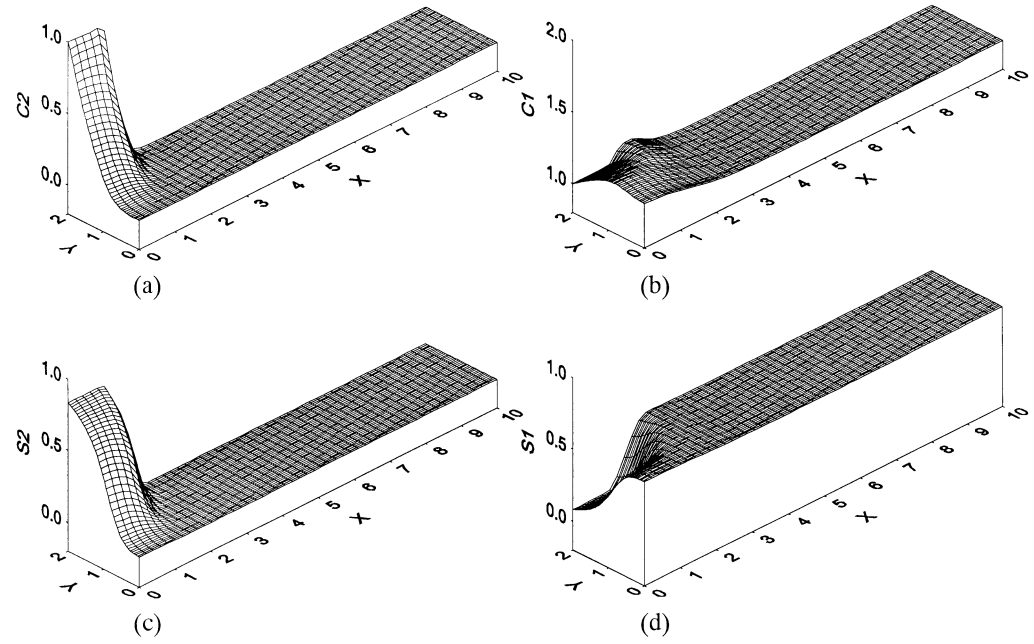

FIGURE 14 Case III: Pure diffusion, concentrations at time $t = 10$.

In all the three cases, the Courant number used equals 1. No time step fails in any analysis. This clearly demonstrates that the TEPG method works well for problems with the Peclet number varying from infinite to zero, without the need for adjusting the Courant number. Although it is not shown here, test runs confirms that the accuracy of the numerical results is not significantly influenced by the actual Courant number used in the analysis.

IV. Conclusion

A two-dimensional finite element method for the solution of the advective-dispersion transport equation with competitive contaminant sorption in soils is presented. The method is based on the one-dimensional Transport-Equilibrium Petrov–Galerkin (TEPG) methods presented by Sheng and Smith [1]. The solution strategy is based on solving the transport and equilibrium equations separately and then seeking convergence between the two systems by iteration. A number of significant refinements are presented in this article, including upwind weighting for a heterogeneous field of fluid velocity, including chemical equilibrium equations for both adsorption and for ion exchange, automatic time stepping and an investigation of strategies for improving the efficiency of the code. It was found that the optimal solution method is one where the system of transport equations are solved simultaneously for all nodes, but independently for each component, while the system of equilibrium equations are solved simultaneously for all components, but independently for each node. By adopting this solution strategy, the TEPG method does not require excessive CPU memory or CPU time as the numbers of nodes and components increase.

For the example problems investigated, it has been demonstrated that the iterative TEPG method works well for two-dimensional transport problems coupled with nonlinear equilibrium processes, in terms of accuracy, robustness, and efficiency, providing the Peclet number is not too high. When the Peclet number is very large, the solution gives results that appear qualitatively correct, but numerical dispersion smooths shock fronts. However, the method has been shown to be capable of predicting important features during the transport of competitive components, including multiple plateaus developed during advection dominated problems involving competitive sorption of multiple components.

An important advantage of the method is that, with error control through an automated time stepping scheme, its accuracy is not significantly influenced by the time step size chosen by the analyst (i. e., the Courant number). For the example problems investigated, the predicted concentrations appear to be accurate for dispersion/diffusion dominated problems. In terms of robustness, this method works well for problems varying from pure advection to pure diffusion.With the optimal upwind weighting, it is not necessary to use very small time steps for pure advection problems. In terms of efficiency, the convergence rate of the TEPG method is relative fast. With a moderate convergence tolerance (10^{-2}) and a normal Courant number ($1 \sim 2$), the method typically requires two or three iterations between the transport and equilibrium equations for each time step.

Although the focus of this article was on nonlinear chemical equations describing ion adsorption and exchange, the general strategy of the TEPG method is also applicable to more general geoenvironmental engineering transport problems. This will form the focus of our next article.

Acknowledgments

The authors wish to thank Professor Scott W. Sloan at the University of Newcastle, Australia, for fruitful discussion.

References

[1] **D. Sheng and D.W. Smith,** Numerical modeling of competitive components transport with nonlinear adsorption, *International Journal for Numerical and Analytical Methods in Geomechanics*, **24**, pp. 47–71, (2000).

[2] **G. Sposito,** *The Chemistry of Soils*, Oxford University Press, New York, (1989).

[3] **A.W. Adamson,** *Physical Chemistry of Surfaces*, 4th edition, John Wiley & Sons, New York, (1982).

[4] **D. Sheng and D.W. Smith,** Analytic solutions to the advective contaminant transport equation with nonlinear sorption, *International Journal for Numerical and Analytical Methods in Geomechanics*, **23**, pp. 853–879, (1999).

[5] **C.W. Jeong and K.J. Lee,** Propagation of concentration waves through a sorption medium with simultaneous ion exchange and electrolyte adsorption, *Waste Management*, **12**, pp. 61–73, (1992).

[6] **J. Rubin and R.V. James,** Dispersion-affected transport of reacting solutes in saturated porous media: Galerkin method applied to equilibrium-controlled exchange in unidirectional steady water flow, *Water Resources Research*, **9**(5), pp. 1332–1356, (1973).

[7] **A.A. Jennings, D.J. Kirkner, and I.L. Theis,** Multicomponent equilibrium chemistry in groundwater quality models, *Water Resources Research*, **28**(4), pp. 1089–1096, (1982).

[8] **G.A. Cederberg,** A groundwater mass transport and equilibrium chemistry model for multicomponent systems, *Water Resources Research*, **21**(8), pp. 1095–1104, (1985).

[9] **F.W. Lewis, C.I. Voss, and J. Robin,** Solute transport with equilibrium aqueous complexation and either sorption or ion exchange: Simulation methodology and applications, *Journal of Hydrology*, **90**, pp. 81–115, (1987).

[10] **A.L. Walter, E.O. Frind, D.W. Blowes, C.J. Ptacek, and J.W. Molson,** Modeling of multicomponent reactive transport in groundwater 1. Model development and evaluation, *Water Resources Research*, **30**, pp. 3137–3148, (1994).

[11] **O.C. Zienkiewicz and R.L. Taylor,** *The Finite Element Method*, 4th edition, Vol. 2, McGraw–Hill book Company, London, (1991).

[12] **G.T. Yeh and V.S. Tripathi,** A critical evaluation of recent developments in hydrogeochemical transport models of reactive multichemical components, *Water Resources Research*, **25**(1), pp. 93–108, (1989).

[13] **R.H. Abrams and K. Loague,** A compartmentalized solute transport model for redox zones in contaminated aquifers, 1. Theory and development, *Water Resources Research*, **36**(8), pp. 2001–2013, (2000).

[14] **R.K. Rowe, R.W. Quigley and J.R. Booker,** *Clayey Barrier Systems for Waste Disposal facilities*, E and FN Spon, (Chapman Hall), London, England, (1995).

[15] **V. Murali and L.A. Aylmore,** Competitive adsorption during solute transport in soils: 1. mathematical models, *Soil Science Society of American Journal*, **135**(3), pp. 143–150, (1983).

[16] **R.D. Harter and D.E. Baker,** Application and misapplications of the Langmuir equation to soil adsorption phenomena, *Soil Science Society of American Journal*, **41**, pp. 1077–1080, (1977).

[17] **S.W. Sloan,** Substepping schemes for the numerical integration of elastoplastic stress-strain relations, *International Journal for Numerical Methods in Engineering*, **24**, pp. 893–911, (1987).

[18] **F. Helfferich and G. Klein,** *Multicomponent Chromatography, Theory of Interference*, Marcel-Dekker, New York, (1970).